Modulation of the Diurnal Cycle of Rainfall Associated with the MJO Observed by a Dense Hourly Rain Gauge Network at Sarawak, Borneo

HIRONARI KANAMORI AND TETSUZO YASUNARI*

Hydrospheric Atmospheric Research Center, Nagoya University, Nagoya, Japan

KOICHIRO KURAJI

Ecohydrology Research Institute, Graduate School of Agricultural and Life Sciences, The University of Tokyo, Tokyo, Japan

ABSTRACT

This study investigates spatiotemporal characteristics of the diurnal cycle (DC) of rainfall over Sarawak in northwest Borneo Island, associated with large-scale intraseasonal disturbances represented by the Madden–Julian oscillation (MJO). This is accomplished using a dense hourly rain gauge network and satellite data. The spatial pattern of the DC is classified into two major groups, coastal and interior regions, based on remarkable differences in rainfall peak times and amplitudes. Amplitudes of the DC and daily rainfall amount increase in active MJO phases at all sites, but the MJO has a stronger effect in the coastal region than the interior region. This modulation of rainfall by the MJO disturbance is largely attributed to rainfall frequency in the interior region, but to both frequency and intensity of rainfall in the coastal region. The low-level westerly wind anomaly enhances convergence, the land–sea breeze, and a midnight rainfall peak in the coastal region during the active MJO phase. Analysis of moisture flux divergence and moist static instability suggests the different dynamics of this modulation of the DC between coastal and interior regions.

1. Introduction

The climate of the Maritime Continent (MC) is characterized by heavy rainfall throughout the year and is an essential atmospheric heat source in Earth's climate system (Ramage 1968). This unique environment, with its complex distribution of islands in the world's warmest ocean pool, favors the development of deep and frequent convection. The major islands in the MC are important in the hydrologic cycle of this region, through complex circulation patterns generated by land–sea contrasts (Neale and Slingo 2003). Land surfaces generate localized convection and lead to formation of active cloud/precipitation systems. There is especially heavy rainfall and deep convection over Borneo, the largest and most central island of

the MC, strongly associated with large-scale tropical disturbances, such as the 30–60-day intraseasonal oscillation represented by the Madden–Julian oscillation (MJO; Madden and Julian 1971, 1972, 1994), Borneo vortex, and cold surge during boreal winter (Chang et al. 2005a).

The MC also has a pronounced diurnal cycle (DC) of convection and rainfall, associated with surface thermal contrast between islands and surrounding oceans. The DC of convection can develop into organized cloud systems, given the very moist tropical atmosphere. Previous studies show a pronounced DC of convection with late afternoon-to-evening maxima over land and nighttime-to-morning maxima over the surrounding seas (Houze et al. 1981; Murakami 1983; Williams and Houze 1987; Nitta and Sekine 1994; Chen and Takahashi 1995; Ohsawa et al. 2001; Yang and Slingo 2001; Neale and Slingo 2003; Kikuchi and Wang 2008). In the boreal winter monsoon period, land breezes converge with northeasterly monsoons to generate offshore convection and heavy rainfall between midnight and morning over western Borneo (Houze et al. 1981).

Rainfall variability appears to be influenced by the seasonal cycles of the summer and winter monsoon,

---

* Current affiliation: Research Institute for Humanity and Nature, Kyoto, Japan.

Corresponding author address: Hironari Kanamori, Hydrospheric Atmospheric Research Center, Nagoya University, Furo-cho, Chikusa-ku, Nagoya 464-8601, Japan.
E-mail: kanamori@hyarc.nagoya-u.ac.jp

particularly over ocean and coastal areas of the western MC (Chang et al. 2005b). On the other hand, the seasonal cycle of rainfall is relatively weak, particularly over Borneo in the MC equatorial area (Kumagai et al. 2005). In this area, the MJO is a remarkable feature of atmospheric circulation and moist convection, which fundamentally modulates heavy rainfall there (Madden and Julian 1994; Zhang 2005). Disturbances on this time scale mainly control the atmospheric heat source, releasing a significant amount of latent heat (Lin et al. 2004). Therefore, interaction of the DC of rainfall (DCR) with the MJO is an important issue for understanding local and regional rainfall processes, and for predictability of the global climate.

Previous studies have reported the impact of the MJO on the DC. Chen and Takahashi (1995) examined the land–sea contrast of the cumulus convection DC during the active/break phase of the MJO over the South China Sea, using equivalent blackbody temperature from a geostationary meteorological satellite (GMS), suggesting that the DC of convection is suppressed in the MJO active phase over the MC. A similar result was reported over the Tropical Ocean Global Atmosphere Coupled Ocean–Atmosphere Response Experiment (TOGA COARE) region, using GMS and radar reflectivity (Sui and Lau 1992; Sui et al. 1997). However, an analysis of the Tropical Rainfall Measuring Mission (TRMM) 3B42 product merged with infrared (IR) radiation data suggests the opposite (Tian et al. 2006). Using TRMM 3B42 and 3G68 datasets, Rauniyar and Walsh (2011) showed that rainfall rate is enhanced over the ocean (islands) during active (suppressed) MJO days. Ichikawa and Yasunari (2006), using TRMM precipitation radar (PR) data, identified a different propagation feature over Borneo associated with large-scale circulation field changes related to MJO disturbances. Thus, the effect of the MJO on the DC is still controversial.

The characteristics of the DC in relation to MJO active phases (with large-scale cloud disturbances) or break phases (without such disturbances) are a matter of keen interest, but the TRMM dataset cannot provide information on temporal evolution. One controversial but critical question is whether the DCR over the MC is affected solely by MJO disturbances. Regarding this issue, we must be careful to use rainfall rate based on convection intensity [e.g., equivalent blackbody temperature or outgoing longwave radiation (OLR)], since heavy rainfall frequently occurs from low-level stratiform clouds associated with cloud/precipitation systems over the major MC islands (e.g., Ichikawa and Yasunari 2006). In addition, it was suggested that the DCR, which is influenced by variation of large-scale, low-level circulations, differs from the coast to the interior of the island

(Ichikawa and Yasunari 2006). Rainfall data from a dense ground-based network, if available, are advantageous in tackling this issue. Some indices of the rainfall rate DC (e.g., rainfall frequency and intensity), in addition to rainfall amount, should also be examined to describe characteristics of the DC in this region.

Seasonal and interannual variability of rainfall based on rain gauge datasets has been identified, for the Indonesian territory of the MC region (Hamada et al. 2002, 2008), Borneo (Gomyo and Kuraji 2006), and the Malay Peninsula and Borneo (Oki and Musiake 1994; Ohsawa et al. 2001). Oki and Musiake (1994) also showed a windward shift of coastal morning maxima of precipitation against the predominant monsoon winds, based on hourly rain gauge data along the shoreline. The effect of the MJO on the DCR over the MC has not been investigated, since dense hourly rain gauge data from the coastal to the interior region of the island are required to do this.

This study examines how the DCR, particularly over the major MC islands, is affected by MJO disturbances, along with its time–space characteristics over the ocean, coastal region, and interior of the island. This, in turn, should deal with the question of how the original MJO cloud system from the Indian Ocean is modified through the DC over the major MC islands. We used a dense hourly rain gauge network across the Malaysian state of Sarawak in western Borneo. Various characteristics of the interaction between the DC of land and ocean systems are also addressed, using TRMM data. Section 2 describes datasets and methods of analysis of hourly rain gauge rainfall used in the study. Section 3 examines general features of DC characteristics, using in situ data and TRMM over the region. Effects on the MJO on rainfall, based on daily rainfall data, are shown in section 4. Impacts of the MJO on the DC based on rainfall amount, frequency, and intensity are described in section 5. The DC of large-scale circulation associated with modulation of the DCR is presented in section 6. Section 7 gives a summary and discussion.

2. Data and methods

a. Daily and hourly rain gauge data

Daily and hourly rainfall data from 50 (almost uniformly distributed) rain stations in Sarawak, Malaysia, Borneo from 1999 to 2003 (5 years of data) were compiled by the Department of Irrigation and Drainage, Sarawak and the Malaysian Meteorological Department. These stations have rainfall datasets with hourly (19 stations) or daily (30 stations) temporal resolution. We also used hourly rain gauges in Lambir Hills
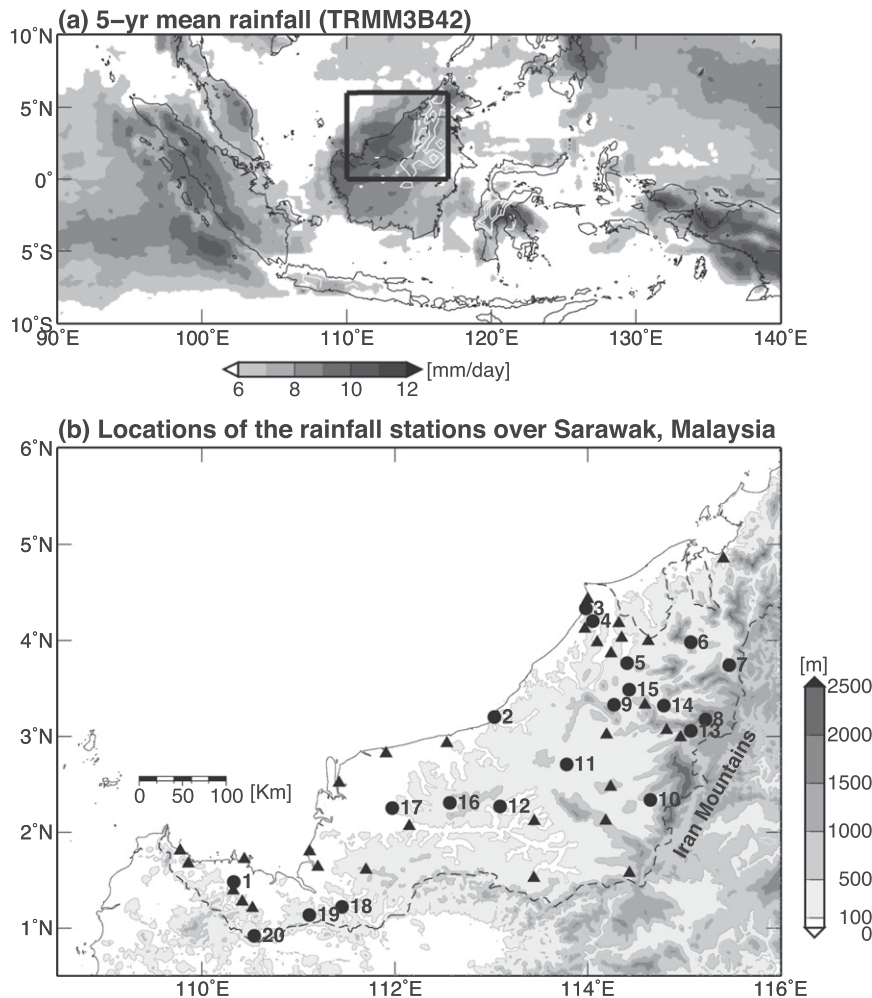
(a) 5–yr mean rainfall (TRMM3B42)

(b) Locations of the rainfall stations over Sarawak, Malaysia

FIG. 1. (a) Distribution of 5-yr mean daily rainfall amounts over Maritime Continent using TRMM 3B42 datasets from 1999 to 2003. Orography is shown by white contour with interval 500 m, beginning at 500 m. (b) Locations of 30 daily rainfall stations (black triangles) and 20 hourly rainfall stations (black circles) in Sarawak, Malaysia. Numbers correspond to hourly rain gauges described in Table 1. The rectangular box shows where area-mean OLR time series were calculated.

National Park (N. P.; 4°20′N, 113°50′E), which is about 12 km from the nearest coast. Figure 1b shows locations of both the daily and hourly rainfall stations. Table 1 shows more detailed information on the 20 hourly rainfall stations, which are at altitudes less than 1000 m above sea level to the west of the Iran Mountains. To focus on the DC, we calculated 3-hourly running means at all stations. Times of maximum and minimum rainfall are directly derived from the DC of these data (Ohsawa et al. 2001). We determined the hours of maximum and minimum rainfall that were more or less than the daily mean rainfall. We defined the largest maximum rainfall peak as a maximum peak. This method detected a semi-diurnal cycle, with two maximum and two minimum

rainfall peaks, at some stations. The larger maximum rainfall was called the first maximum rainfall peak and the other the secondary maximum rainfall peak. We also defined the amplitude of the DCR as the difference in rainfall amount between the maximum rainfall and daily mean.

b. TRMM dataset

The influence of the MJO on the DC over the Sarawak region was investigated primarily based on rain gauge data. However, these data are limited to land areas. The DCR is driven by thermal contrast between the land and surrounding ocean. We used the TRMM 3B42, version 6 (Huffman et al. 2007) rainfall dataset to investigate

TABLE 1. Locations and details for 20 hourly rainfall stations.

No.	Station name	Lon (°E)	Lat (°N)	Distance (km)	Elev (m)	Category
1	Kuching	110.33	1.48	20	22	C-1
2	Bintule	113.03	3.20	2	3	C-2
3	Miri	113.98	4.33	3	17	C-3
4	Lambir Hills N. P.	114.05	4.20	15	59	C-3
5	Lama, Long	114.40	3.76	75	75	C-4
6	Seridan, Long	115.06	3.98	101	192	C-4
7	Bareo	115.46	3.74	148	1005	C-4
8	Lio Matu	115.22	3.17	186	285	C-5
9	Subing, Long	114.27	3.33	95	35	C-5
10	Lidam, Long	114.65	2.34	201	515	C-5
11	Belaga	113.78	2.71	98	40	C-5
12	Merit, Nanga	113.09	2.27	96	30	C-5
13	Moh, Long	115.07	3.05	181	250	C-6
14	Akah, Long	114.79	3.32	139	135	C-6
15	Pilah, Long	114.43	3.49	95	56	C-6
16	Sungai Arau	112.57	2.31	76	82	C-7
17	Sibu	111.97	2.25	70	8	C-7
18	Sri Aman	111.45	1.25	65	10	C-7
19	Pantu	111.11	1.14	45	21	C-7
20	Bunan Gega	110.54	0.92	77	70	C-7

spatial distribution of rainfall over Borneo and the surrounding ocean. This dataset is created by blending passive microwave data collected by the TRMM Microwave Imager (TMI), Special Sensor Microwave Imager (SSM/I), Advanced Microwave Scanning Radiometer for Earth Observing System (AMSR-E), Advanced Microwave Sounding Unit B (AMSU-B), and IR data acquired by the international constellation of geosynchronous Earth orbit (GEO) satellites, and based on calibration by the precipitation estimate of the TMI–PR combined algorithm. This product is created by merging the monthly accumulation with the monthly accumulated Climate Assessment and Monitoring System (CAMS) and Global Precipitation Climatology Centre (GPCC) rain gauge analysis. A description of the 3B42 algorithm is provided online (http://trmm.gsfc.nasa.gov/3b42.html). This dataset covers both temporally and spatially consecutive data in the domain from 50°S to 50°N every 3 h, with horizontal resolution 0.25° × 0.25°.

c. Other datasets

To examine interactions between rainfall variability over Sarawak and the larger surrounding area, including those with the atmospheric circulation field, we used Japanese 25-yr Reanalysis (JRA-25) data on a 1.25° latitude–longitude grid (Onogi et al. 2007). Daily interpolated outgoing longwave radiation datasets from the National Oceanic and Atmospheric Administration (NOAA) Climate Prediction Center (CPC) (Liebmann and Smith 1996) from a 5-yr period (1999–2003) were also used. These datasets have spatial resolutions of 2.5° × 2.5°.

3. General features of rainfall activity over Borneo

Figure 1a shows the spatial distribution of 5-yr mean daily rainfall over the MC from TRMM. The overall spatial pattern shows heavier rainfall over land areas (e.g., Sumatra, New Guinea, and Borneo) and less over surrounding oceans and open sea. The area of heaviest rainfall on Borneo appears in its western part (Sarawak). Figure 2a shows the spatial distribution of 5-yr mean daily rainfall amounts over Sarawak from the 50 rainfall stations. This areal contrast in rainfall differs from area to area (Fig. 1a). Rainfall data from TRMM generally tend to be underestimated over land relative to that from in situ data (Nair et al. 2009; Yuan et al. 2012). These works also show that this tendency varies by area over the land, and the spatial pattern of rainfall is similar in both datasets. Rainfall amount from TRMM tends to overestimate (underestimate) in coastal (interior) areas relative to in situ data. The greatest rainfall appears in inland areas of the western mountains, and the least in the northern coastal area—at Miri (No. 3; numbers refer to locations in Table 1 and Fig. 1b) and Lambir Hills N. P. (No. 4) (rainfall in the two regions differs by a factor greater than 2). Figure 2b shows spatial distributions of phase and amplitude of the 5-yr mean DCR from hourly rainfall data; maxima are indicated by the directions of arrows and amplitudes by their lengths. On the whole, an afternoon-to-night maximum [1600–2100 local time (LT); all subsequent times are LT] is dominant in most regions. The peak time in southwest Sarawak (around 110° to 112°E) is during the evening (1600–1700),
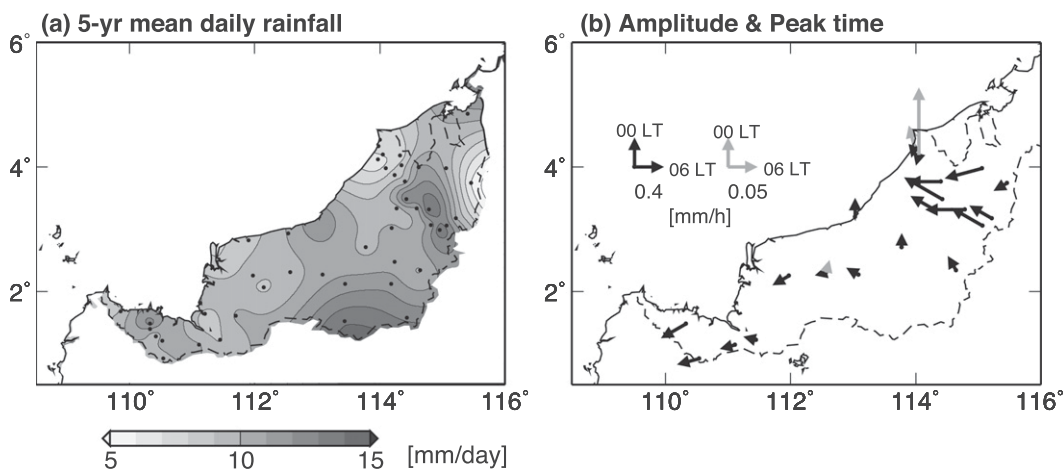
(a) 5-yr mean daily rainfall

(b) Amplitude & Peak time

FIG. 2. (a) Distribution of 5-yr mean daily rainfall amount (mm day^{-1}) over Sarawak, using 50 rainfall stations from 1999 to 2003. (b) Time of maximum rainfall of 20 hourly rainfall stations, for 5-yr mean. Vector orientation indicates local time of maximum rainfall, and length indicates deviation from daily mean (mm h^{-1}). Black and gray vectors represent primary and secondary maxima, respectively, which are defined from daily mean rainfall.

and that of northeast Sarawak (around 114° to 116°E) is at night (1900–2100). Maximum rainfall is at midnight (0000) in Bintulu (No. 2), which is closest to the coast. In addition, Miri (No. 3) and Lambir Hills N. P. (No. 4), a few kilometers from the coastline in the northeast area, also experience rainfall near midnight (at 2300 and 0000, respectively). Sungai Arau (No. 16), about 30 km from the nearest coast, and Belaga (No. 11), in central Sarawak, have rainfall peaks at 0100 and 0000, respectively. The rainfall amount and time of occurrence of maximum diurnal rainfall exhibit large regional differences over Sarawak.

To classify the DCR pattern more objectively, Ward's cluster analysis was applied to 5-yr mean hourly rainfall, which showed that the spatial pattern of rainfall in the region can be divided into seven categories (Table 1): the southwest category (C-1) with one station; the coastline category (C-2) with one station; the northeast coastal area (C-3) with two stations; the interior plain to mountain categories (C-4, C-5, and C-6) with three, five, and three stations, respectively; and the central plain category in the south (C-7) with five stations (Fig. 3). These seven rainfall classifications based on the mean DC pattern are similar to the categorized spatial pattern of rainfall using climatological pentad means for this region (Gomyo and Kuraji 2006). This suggests that seasonal and annual rainfall patterns depend on the regional DC pattern. Figure 3 shows the DC of 5-yr mean rainfall for the seven categories, which are averaged for the stations in each category. The DCs in all categories show a time of minimum rainfall during 0900–1100, indicating that rainfall is suppressed in the morning over the entire

region. The afternoon-to-nighttime rainfall peak propagates from coastal to interior areas in the following order from 1300 to 2100: C-3, C-1, C-4, C-7, C-6, and C-5 (Fig. 2b). In the coastline and coastal categories, the midnight-to-morning rainfall peak is apparent at C-2 and C-3, occurring at 2300 and 0000, respectively. The DC at C-3, which is a few kilometers from the coastline, shows features of both coastal (midnight to morning peak) and interior (afternoon to nighttime peak) areas. Additionally, the inland categories (C-4 to C-7) show different times of DC peak and amplitude from region to region, although all peak times are in the late afternoon to nighttime. Although detailed characteristics of the DC patterns vary greatly by region, presumably because of complex terrain, characteristics of the DCR (time of maximum rainfall and its amplitude) can be grouped into two types: coastal (C-1 to C-3) and interior regions (C-4 to C-7).

The time of maximum rainfall strongly depends on distance from the coast. Scatter diagrams show the dependence of time of maximum rainfall in the 5-yr dataset on distance from the coastline (Fig. 4). The regression line and correlation coefficient refer only to the afternoon-to-nighttime (1200–2200) rainfall peaks, which are shown as crosses. The relationship between distance from the coast and time of maximum afternoon-to-nighttime rainfall shows significant ($p < 0.05$) correlation ($r = 0.74$). Only a few stations, within about 30 km of the coastline, have double rainfall peaks (i.e., a large afternoon maximum and small midnight-to-morning maximum). This indicates that these near-coast areas receive rainfall from both afternoon-to-nighttime and midnight-to-morning systems.
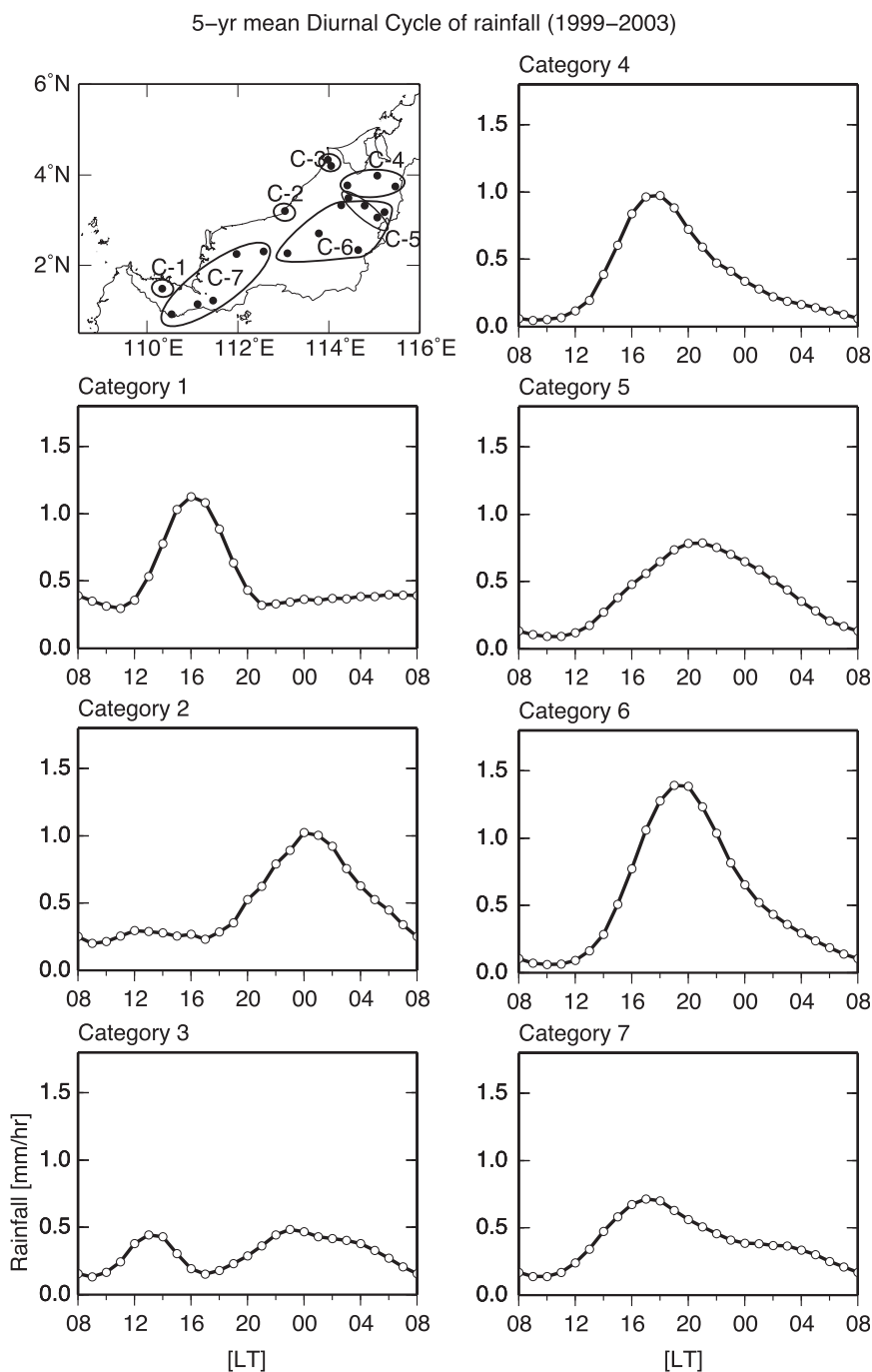
5–yr mean Diurnal Cycle of rainfall (1999–2003)

FIG. 3. The 5-yr mean DCR for the seven categories. Thick black solid lines indicate average rainfall of all stations in each category. Numbers correspond to rain stations described in Table 1. (top left) Map showing location of the seven categories over Sarawak.

4. Effects of MJO on daily rainfall variation

Daily variation of the DCR over Sarawak is thought to be associated with variation in the large-scale circulation field. The seasonal cycle of rainfall over Borneo is weak compared with other tropical areas, as revealed by relatively low spatial resolution OLR data (Matsumoto 1997; Kumagai et al. 2005). However, Gomyo and Kuraji (2006) found a distinct climatological seasonal cycle of rainfall in southern Sarawak (approximately corresponding to C-1 and C-7), using rain gauge data. They suggested that this seasonal cycle is caused by topographic effects.
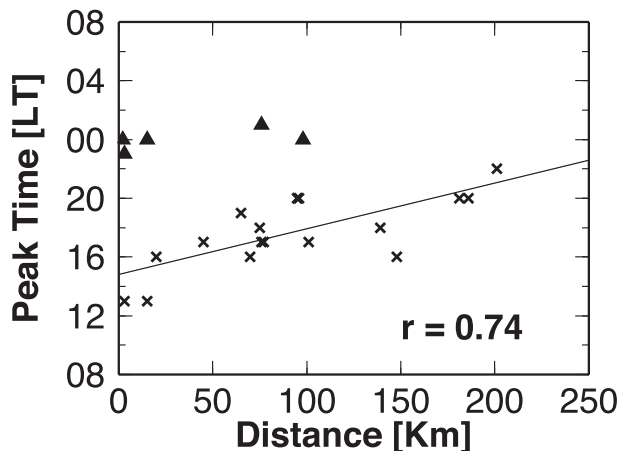
FIG. 4. Scatter diagram of peak time of rainfall vs distance from the coast, for 5-yr mean DC of the 20 hourly stations. Crosses and triangles indicate afternoon-to-nighttime and midnight-to-morning rainfall peaks, respectively. Regression line and correlation coefficient indicate correlation between afternoon-to-nighttime peaks and distance from the coast.

Figure 5 shows a time series of average daily rainfall at the 50 stations from 1999 to 2003. There is a weak seasonal cycle, with relatively heavy rainfall in the boreal winter. The northeasterly monsoon flow enhances rainfall and convective activity particularly over the South China Sea (Chang et al. 2005a,b). The coastal region of the southern Sarawak (C-1 and C-7) is strongly affected by this seasonal cycle. The rainfall time series of these stations show distinct intraseasonal variations in addition to the seasonal cycle, which is dominant commonly over the entire Sarawak region. Spectral analysis using the fast Fourier transform (FFT) method was applied to the 5-day running mean daily rainfall from the entire 5-yr (1826 days) period. Figure 5 shows the power spectrum for this time series, revealing a dominant peak around 50 days and a secondary peak from 25 to 30 days. These correspond to the dominant periods of intraseasonal variations of large-scale convection in the MC (Hsu and Lee 2005; Zhang 2005).

Temporal variation in circulation and large-scale convection associated with predominant intraseasonal variations of 50-day period in Borneo was examined by a time-composite technique for the entire 5-yr dataset. OLR data were adopted as a measure of deep convection associated with these MJO-related variations (Chang et al. 2005a). Twenty-six cycles with maximum and minimum events exceeding a standard deviation of 1.0 were selected for the composites, based on 25–70-day bandpass-filtered anomalies of area-averaged OLR time series (0°–6°N, 110°–117°E; rectangular box in Fig. 1a). The 25–70-day OLR 5-yr time series shows significant ($p < 0.05$) negative correlation ($r = -0.50$) with the

25–70-day daily mean rainfall 5-yr time series over the Sarawak region. Fourteen cycles were selected for the composite in boreal summer (April–September) and 12 cycles for boreal winter (October–March). Eight phases make up each cycle. To retain sufficient sample sizes for both phases, active and break phases of MJO scale are defined by the period from phase 1 to 3 and that from phase 5 to 7, respectively.

Using the gauge datasets, the spatial distributions of daily rainfall in active and break phases over Sarawak are shown in Figs. 6a and 6b (cf. Fig. 2a). In the active phase, Sarawak rainfall increases relative to the break phase, although the spatial pattern of large rainfall amounts in the interior mountains and southwest coastal areas does not change greatly in either phase. The largest difference is in the coastal region and foothills of the interior. Rainfall enhancement is particularly extreme near the coast. The spatial distribution of rainfall rate of change from active to break phase shows a clear difference (Fig. 6c). Coastal areas facing northwest show the largest rainfall change from the MJO break to active phase, whereas those facing north show less change. The interior mountain region of the island, with high rainfall, shows even smaller changes. Thus, daily rainfall from gauges increases in the active phase regionwide, but more remarkably in the coastal areas, suggesting a stronger response to the MJO. Like Figs. 6a–c, Figs. 6d and 6e show a spatial distribution of daily rainfall, but the data are derived from the TRMM and cover all of Borneo and surrounding oceans. Overall, in both phases, TRMM overestimated (underestimated) rainfall in coastal (interior) regions, relative to the gauge data. This tendency is likely to hold even for the 5-yr mean DCR (Figs. 1 and 2a). The TRMM shows that rainfall over land and surrounding ocean increases in the active phase. In the surrounding ocean during this phase, the distribution of heavy rainfall area is extensive, from the coastline to open ocean. However, this distribution is limited to near-coastal areas in the break phase. Figure 6f shows the rate of change of TRMM rainfall from break to active phases. This rate is much greater over the ocean than over land. It was found that TRMM rainfall over land underestimates the impact of the MJO on rainfall, compared with that suggested by the gauge data. However, the common indication from both datasets is that the influence of the large-scale MJO on rainfall varies across oceanic, coastal land, and interior land areas.

5. Change of rainfall diurnal cycle associated with MJO

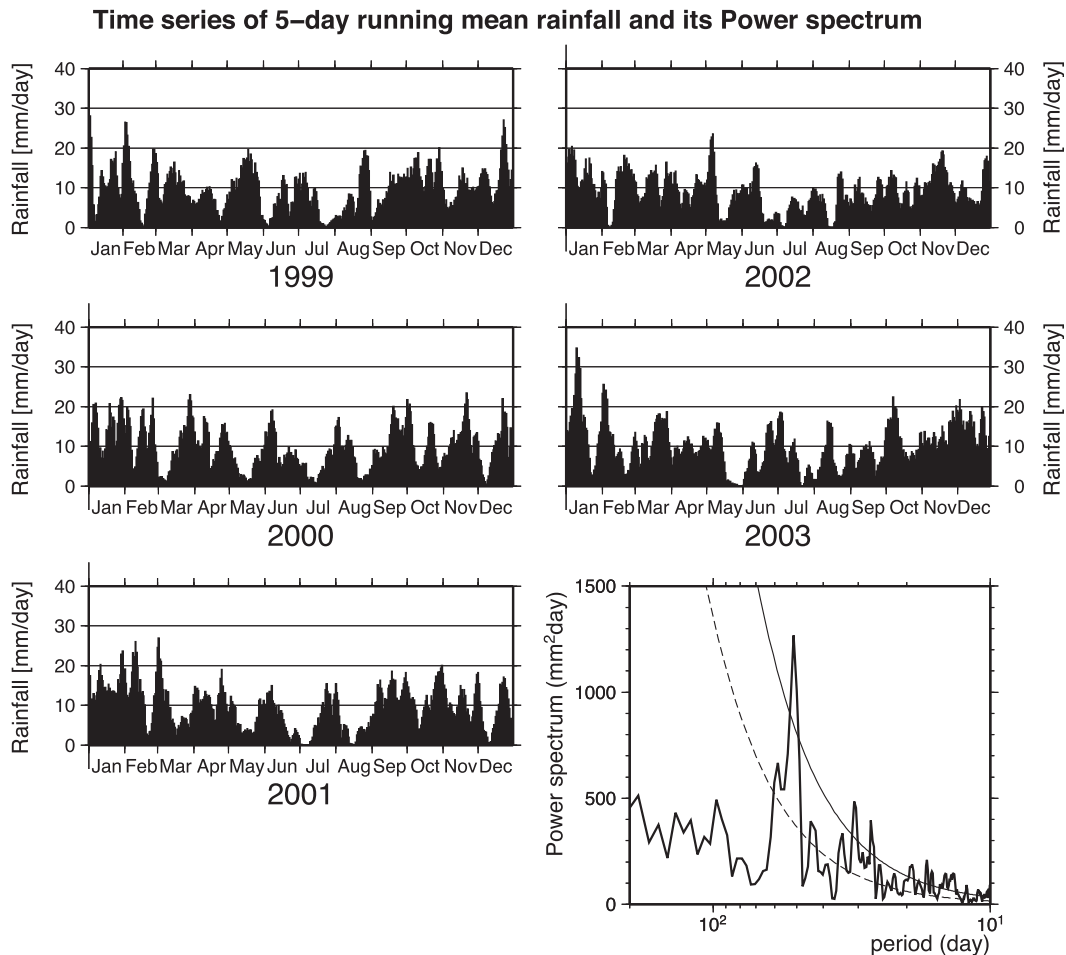Figure 7 shows modulation of the DCR attributed to the global-scale MJO for the seven categories (defined

Time series of 5–day running mean rainfall and its Power spectrum

FIG. 5. Time series of 5-day running mean rainfall (mm day^{-1}), averaged over 1999–2003 from rain gauge observations at 50 stations. (bottom right) The power spectrum of the 5-day running mean rainfall averaged at 50 rainfall stations. Dashed line indicates red-noise spectrum, and solid line shows 95% significance level.

in Fig. 3). All categories show rainfall minima around 1000, as well as the DC in both active and break phases. They also show that hourly rainfall increases between break and active phases (except for minimum rainfall time). In the break phase, the rainfall peak from afternoon to nighttime is between 1200 and 1600 in the coastal categories (C-1 to C-3). This rainfall maximum propagates inland (e.g., C-4 to C-7 show the maximum between 1700 and 2000). The rainfall peak from midnight to morning occurs at 0200 in C-2 and C-3. The second rainfall peak appears at 1400 in C-2, although it is smaller than the other rainfall peaks. C-1 has a second maximum at 0800, although this is not shown in the mean DC. In the active phase, the rainfall peak from afternoon to nighttime in the coastal categories remains unchanged. The DC in the interior categories (C-4 to C-7) indicates a remarkable rainfall increase from the break to active phase. The midnight-to-morning rainfall

maximum is at 0000 in the coastal categories (C-1 to C-3). C-2 has a small secondary rainfall maximum at 1200, although a clear difference is not evident between active and break phases. This rainfall peak appears 2 h earlier during the break phase, although the difference is small. In C-1, the rainfall peak at 0000 in the active phase appears as a secondary rainfall maximum.

In the coastal region (C-1 to C-3), although the afternoon-to-nighttime rainfall maximum is not influenced by the MJO, that from midnight to morning is clearly so influenced. The midnight-to-morning rainfall peak in C-2 doubles from the break to active phase. The rainfall minimum at 1800 (C-2 and C-3), a boundary between the afternoon and midnight-to-morning rainfall systems, is only distinct during the break phase. In interior mountain regions (C-4, C-6, and C-7), the DC phase does not change between active and break phases, whereas its amplitude (rainfall amount) increases (decreases) in the
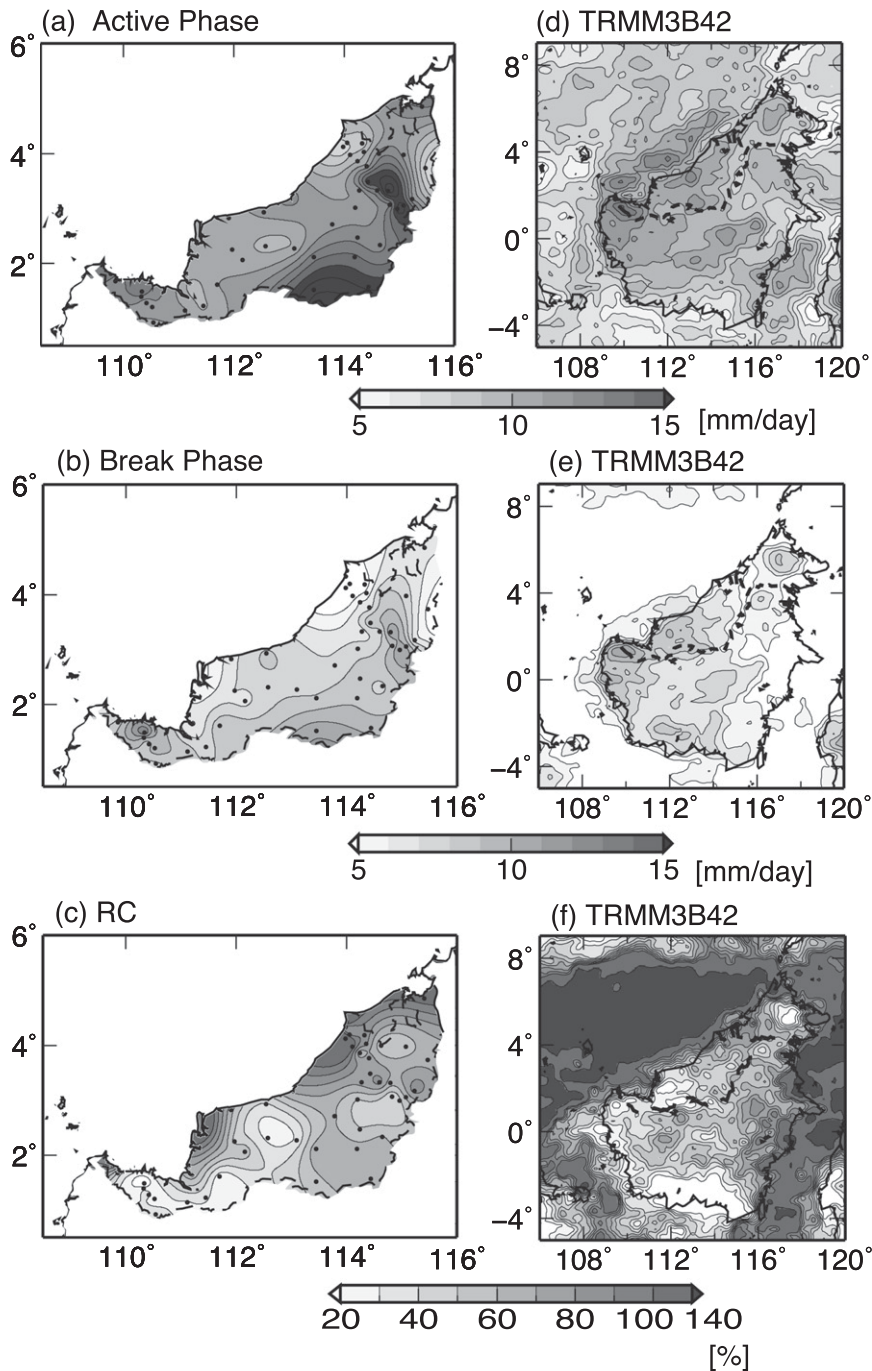
FIG. 6. Composites of daily rainfall in the (a) active and (b) break phase over Sarawak, based on 50 rainfall stations. (c) Spatial distribution of rate of change (%) in rainfall from active to break phase that is defined as [(active phase)/(break phase) − 1] × 100. (d)–(f) As in (a)–(c), but based on TRMM 3B42 data over Borneo and surrounding ocean.

active (break) phase. In addition, the DC in C-5 seems to reflect some DC phase change. It is well known that the DC has a midnight-to-morning rainfall peak over the tropical ocean (Yang and Slingo 2001; Kikuchi and Wang 2008). The midnight-to-morning peak near the coast may

be related to this oceanic peak. In fact, the MJO has more impact on rainfall over the ocean than over land (Fig. 6). As a result, the DC in coastal categories is modulated more strongly by the midnight-to-morning peak over the ocean than peaks in the island interior (C-4 to C-7). The

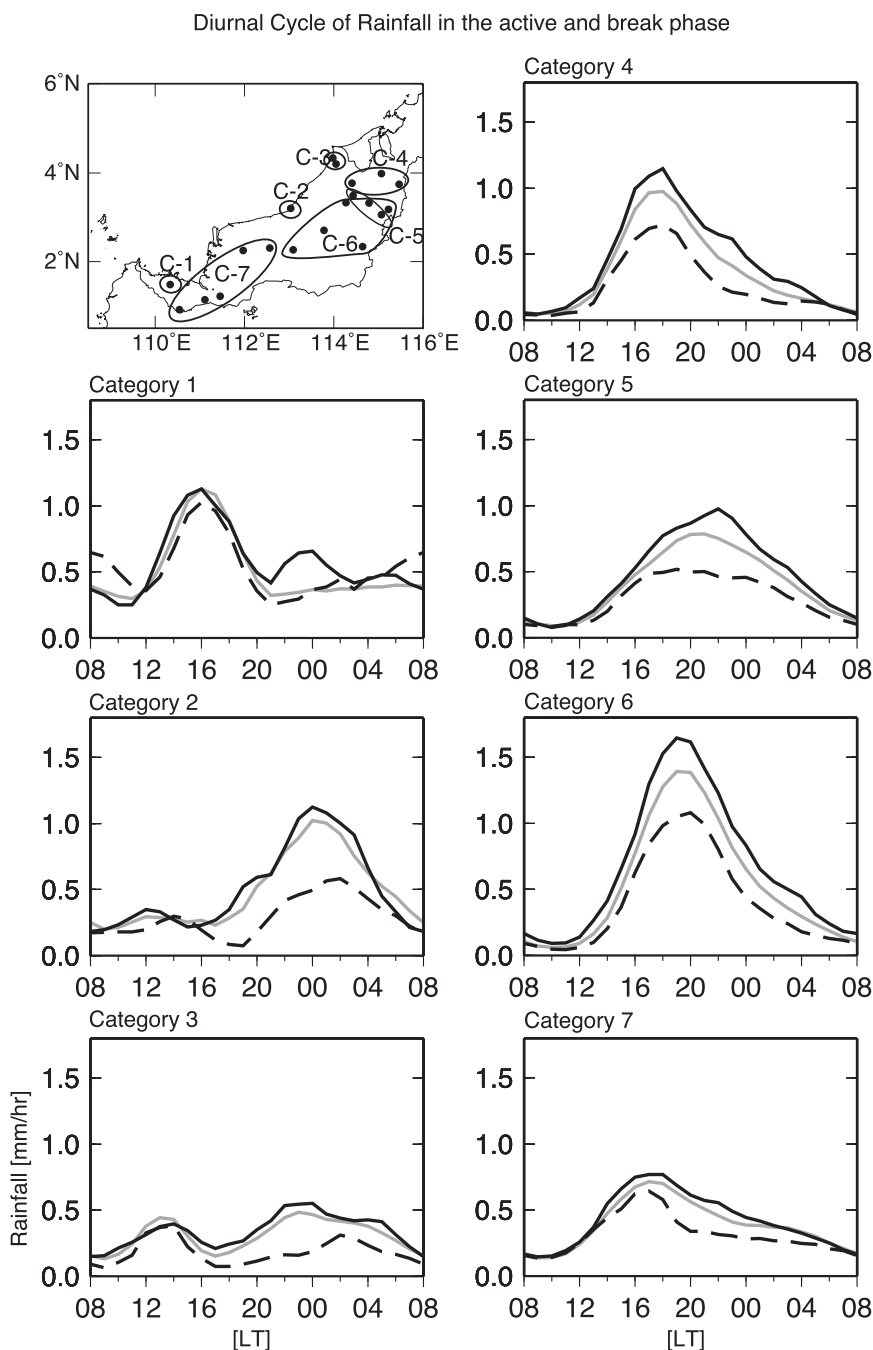Diurnal Cycle of Rainfall in the active and break phase

FIG. 7. Composite of DCR based on gauge data, in both active and break phases for the seven categories. Solid (dashed) line indicates the active (break) phase rainfall in each category. Gray solid line indicates the 5-yr mean DCR, as shown in Fig. 3.

differences of 5-yr mean rainfall in Fig. 3 (gray solid line in Fig. 7) from both phases shows that the DC in coastal regions depends more on the MJO than in the interior. Thus, change of the DCR in terms of amounts and phases from the MJO break to active phase exhibits different characteristics between coastal regions and the interior.

Figure 8 shows the DC of frequency and intensity of the rainfall composite for the seven categories. Rainfall frequency is defined by the number of rainfall days for each hour per total number of days (a percentage), and rainfall intensity is defined by rainfall amount per rainfall event for each hour in both phases, for each station.
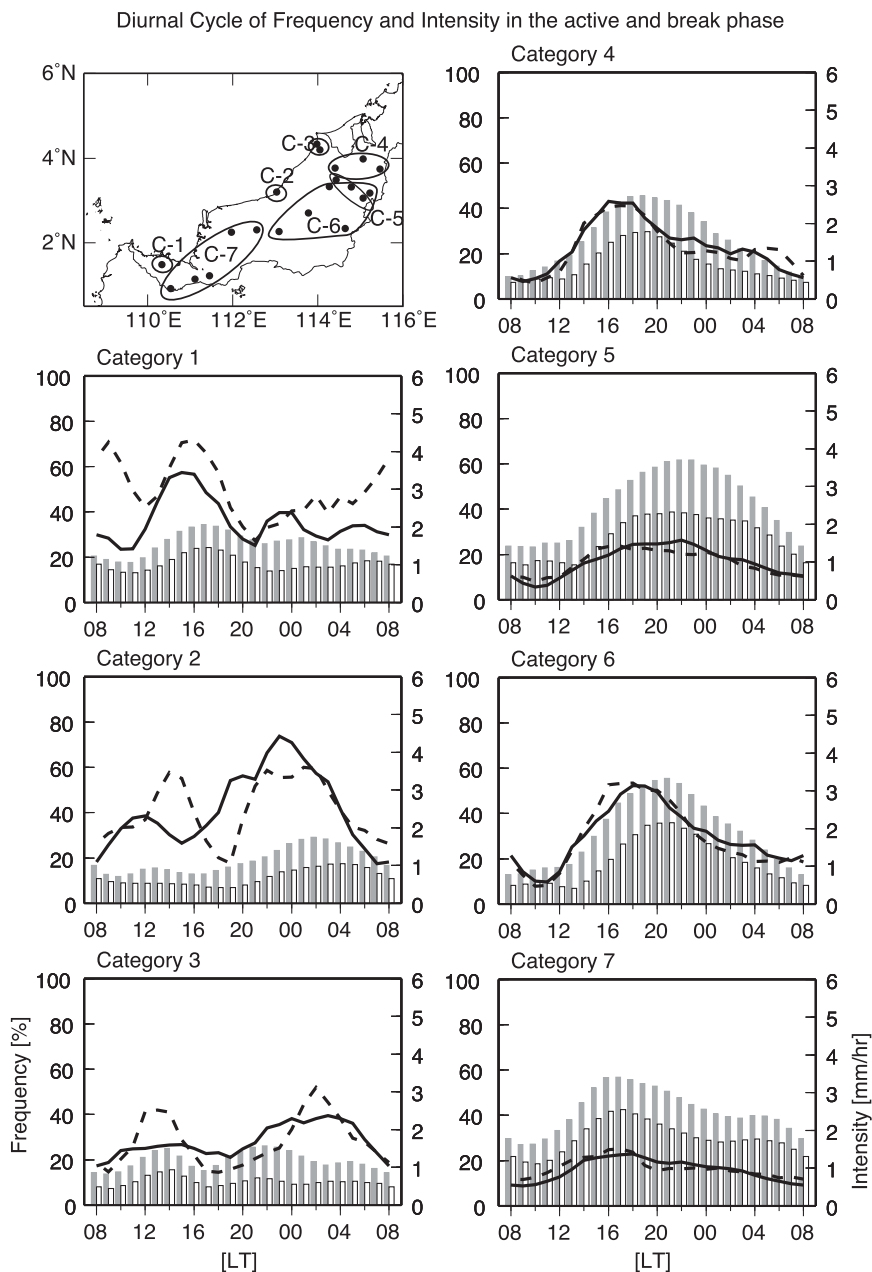
FIG. 8. Composite of DC frequency (%) and intensity (mm h^{-1}) of rainfall for the seven categories. Gray (white) bars indicate frequency of rainfall in the active (break) phase with left axis, and solid (dashed) line indicates intensity of rainfall in the active (break) phase with right axis, respectively.

In all categories, rainfall frequency increases through the day from break to active phases. This tendency is remarkable. Over all interior categories (C-4 to C-7), the DC of intensity does not change between phases. Hence, DC variation in both phases is represented by a change in frequency of rainfall between active and break phases. In the coastal categories (C-1 to C-3), however, the DCR intensity is clearly different between

phases. In the break phase, this DC has large amplitude relative to the active phase. The afternoon-to-nighttime maximum of intensity in the break phase in coastal categories (C-1 to C-3) is stronger than in the active phase. In C-2, the afternoon-to-nighttime peak time of intensity in the break phase is 2 h earlier than in the active phase. This tendency is consistent with rainfall amount, as shown in Fig. 7.
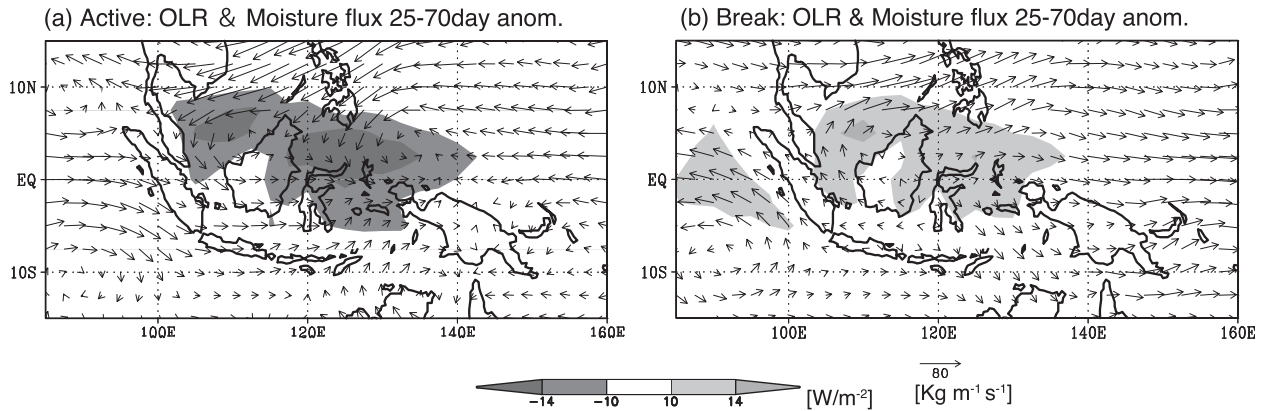
FIG. 9. Spatial distribution of composite anomalies in 25–70-day band, based on OLR area-average time series. OLR (W m^{-2}) and vertically integrated (from surface to 100 hPa) moisture flux vectors (kg m^{-1} s^{-1}) anomalies for the (a) active and (b) break phases.

Therefore, the change of DC between break and active phases in the interior region is explained by change in the DC of frequency. On the other hand, change of the DC in the coastal region is affected by changes both of frequency and of rainfall intensity. The DC in the coastal region is strongly affected by characteristics of the oceanic DC, where the impact of the large-scale cloud systems associated with the MJO is important.

6. Diurnal cycle of large-scale circulation associated with MJO

This section is devoted to discussion on how the DC across the ocean, coastal zone, and interior of Borneo Island is modulated by the MJO. Figure 9 shows a composite map of OLR and vertically integrated moisture flux anomalies for active and break phases. In the active phase, a low OLR anomaly appears over the entire MC, including the South China Sea, Borneo, and particularly the ocean surrounding Borneo. The South China Sea is dominated by a northeasterly moisture flux anomaly in this phase, which depends on the low-level wind. This moisture flux is presumably affected by island topography, and it changes from northeasterly to northwesterly over the equatorial South China Sea between Sumatra and Borneo. As a result, the moisture flux anomaly seems to form a cyclonic circulation, centered over the southwest coast of Borneo. On the other hand, during the MJO break phase in this region, OLR and moisture flux anomalies show suppressed convection and an anticyclonic circulation, almost opposite that of the active phase. It seems that anomalous deep convection systems during the active phase dominate the surrounding oceans more than Borneo.

Throughout one cycle (phases 1 to 8, not shown), negative OLR values (corresponding to cloud systems) propagate eastward, which are coupled with a baroclinic atmospheric structure with strong upper divergence. Simultaneously, low-level wind field anomalies change from westerly to easterly. With maximum rainfall over Borneo, low-level wind field anomalies transition from northeasterly to southwesterly, corresponding to enhanced cyclonic circulation anomalies associated with strengthened large-scale convection over Borneo and surroundings. Thus, rainfall variation in Borneo is modulated by large-scale convective variability, principally related to the MJO. Rainfall during the active phase in the coastal region, which is perpendicular to the westerlies, is strongly influenced by a low-level cyclonic anomaly associated with the MJO (Fig. 9a).

The DCR is mainly controlled by the land–sea breeze, which is in turn controlled by differential thermal heating (Nitta and Sekine 1994; Chen and Takahashi 1995; Yang and Slingo 2001). To examine moisture balance and thermodynamic characteristics of the island-scale convective system associated with the two MJO phases, composites of the DC for vertically integrated moisture flux divergence and atmospheric instability are produced in Fig. 10. The latter variable is defined as the difference of equivalent potential temperature between 850 and 500 hPa. Figures 10a–d show spatial patterns of average fields over Borneo and surrounding oceans at several times of the day (0800, 1400, 2000, and 0200), as represented by means of the active and break phases. It was found that the DCs of these two atmospheric fields are clearly associated with the DCR. Because of strong surface heating by solar radiation and moisture increase in the lower troposphere over land, atmospheric instability is enhanced in the afternoon to evening (1400–2000). Moisture flux divergence dominated by the low-level wind field is related to the land–sea breeze, more prominently on the west coast and interior of Borneo.
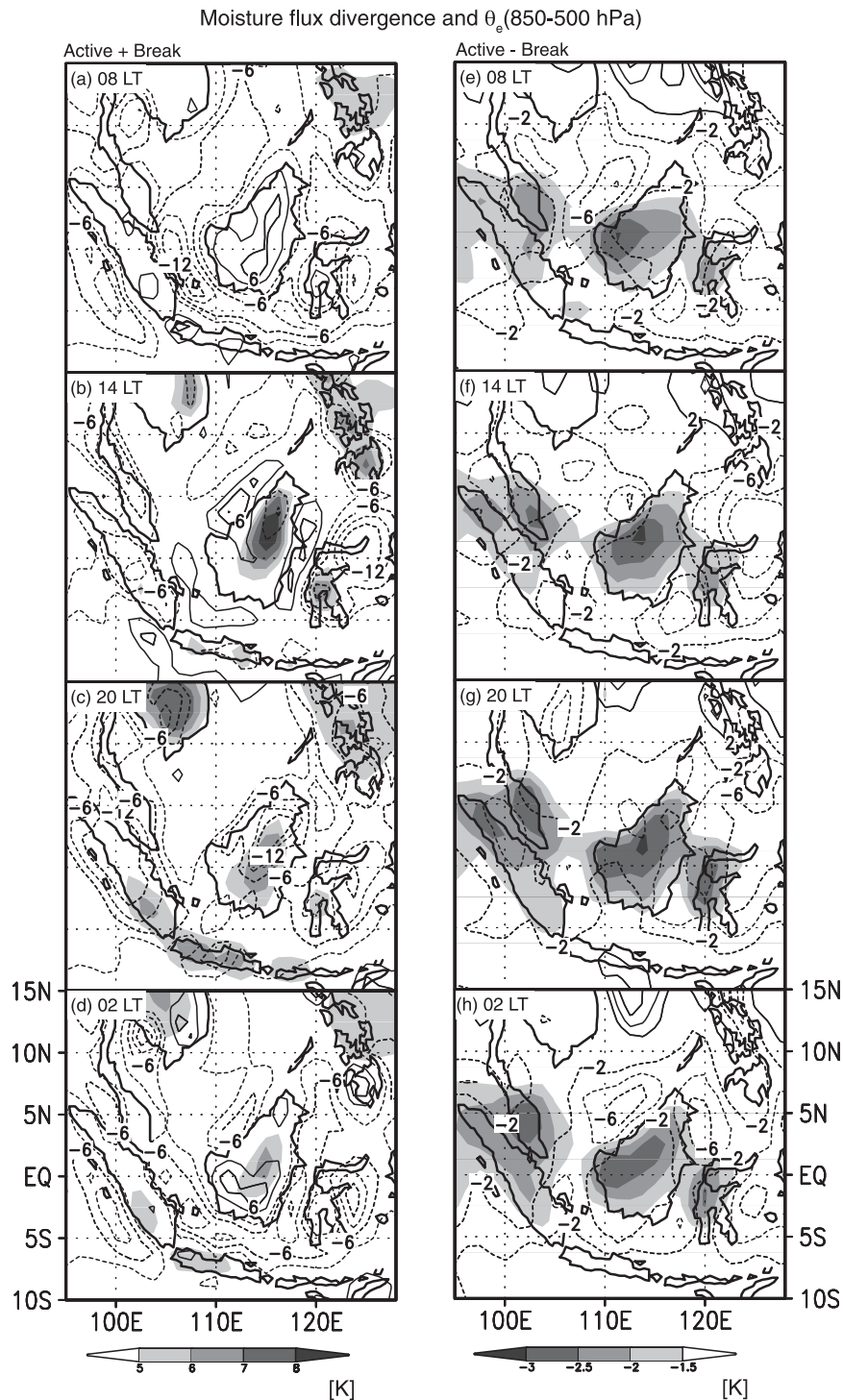
Moisture flux divergence and θ$_e$(850-500 hPa)

FIG. 10. (a)–(d) The DC of vertically integrated (surface to 100 hPa) moisture flux divergence (contour) and atmospheric thermodynamic instability, defined as the difference in equivalent potential temperature θ_e between 850 and 500 hPa [shaded; θ_e (850 hPa) $-$ θ_e (500 hPa)], for the means of active and break phases. (e)–(h) As in (a)–(d), but for the difference between peak active and break phases. For (a)–(d), the contour intervals for moisture flux divergence are -12.0, -9.0, -6.0, -3.0, 3.0 6.0, 9.0, and 12.0 and for (e)–(h), the intervals are -8.0, -6.0, -4.0, -2.0, 2.0, 4.0 6.0, and 8.0. The unit for moisture flux divergence is 10^{-5} kg m^{-2} s^{-1}.

Moisture flux convergence is enhanced over land at 2000 and surrounding ocean at 0200. Differences of these fields from active to break phases are shown in Figs. 10e–h. The DC of these two fields show similar features in both phases, but DC amplitudes modulated by the large-scale atmospheric circulation vary between break and active phases, resulting in more active convection and heavier rainfall over the MC. Moisture flux convergence over the west coast of Borneo is more enhanced from midnight to morning (0200–0800) in the active phase. This seems consistent with the strengthening of convergence between the offshore wind and low-level westerly anomaly related to the active MJO phase (Fig. 9). Furthermore, moisture flux convergence is enhanced throughout the day in the active phase. Water vapor is transported from the ocean further into the interior. This contributes to the frequency increase in the interior from the break to active phase (Fig. 8). In the active phase, as a result of enhanced convective activity, atmospheric instability is suppressed over land through the day. This also suggests that the rainfall increase is attributable to the frequency increase rather than the intensity increase over land.

7. Summary and discussion

The spatial distributions of DCR were subdivided into seven categories, based on phase and amplitude of the DC of 5-yr mean rainfall. The coastal region (up to about 30 km from the coastline) has two rainfall maxima periods—from afternoon to nighttime, and midnight to morning. The interior region has only one maximum, during afternoon to nighttime. These rainfall maxima are likely generated by land–sea temperature contrast and resulting land–sea breeze convection systems (Houze et al. 1981; Nitta and Sekine 1994; Chen and Takahashi 1995; Yang and Slingo 2001). The variable characteristics of DCR between land and ocean over the MC were discussed by Kikuchi and Wang (2008). Here, the DCRs are further categorized into seven subdivisions of the coastal and interior region, based on in situ hourly rainfall data over western Borneo.

We then investigated the impact of large-scale, eastward-moving MJO disturbances of 25–70-day time scale on the DCR in this region. A seasonal cycle of low-level circulation fields (i.e., westerlies in boreal summer and northeasterlies in boreal winter) is dominant across the MC (Chang et al. 2005b). It affects deep convection over the South China Sea and coastal Borneo associated with the MJO through the year. The deep convection also appears associated with the MJO and other synoptic disturbances, which are Borneo vortex and cold surge in boreal winter monsoon (Chang et al. 2005a). The time

series of daily rainfall based on rain gauges over Sarawak, however, shows a relatively weak seasonal cycle and distinct intraseasonal variations of 25–70-day time scale throughout the year. A time–longitude section of OLR along the equator reveals that this intraseasonal variation of rainfall over Sarawak (Fig. 5) is associated with large-scale eastward-moving MJO disturbances, indicating that the MJO disturbances have a strong effect on daily rainfall variation over this region basically throughout the year. The daily rainfall variation is also strongly controlled by the DC. Ichikawa and Yasunari (2006) showed that the DCR over Borneo is modulated by the change of low-level wind anomaly from westerly to easterly, which depends on the phase of the MJO. We also investigated how these MJO disturbances affect the DCR from coastal to interior regions of Sarawak, based on the analysis of the rain gauge dataset of this region.

The rain gauge data show larger rainfall amounts than TRMM 3B42 over land in active phase of the MJO (Fig. 6). This suggests that the TRMM data likely underestimate the MJO effect over land. Some previous studies reported the same tendency in rainfall between satellite and in situ data over the land except the coastal region (Nair et al. 2009; Yuan et al. 2012). Some recent studies also show that the TRMM PR data cannot capture rainfall from shallow clouds in mountainous regions adequately, associated with local mountain–valley circulations (Kwon et al. 2008; Kubota et al. 2009). The spatial pattern of gauge rainfall clearly shows the increase from the coastal to interior region in the break to active MJO transition. On the other hand, TRMM 3B42 data show that coastal rainfall changes are synchronized with those over the nearby ocean, where the MJO disturbance effect is stronger than in the interior. The tendency becomes clearer in the boreal summer than in the boreal winter (not shown), because the other synoptic disturbances such as Borneo vortex and cold surges are enhanced in the boreal winter (Chang et al. 2005a). However, the effect of MJO on the DCR appears in the both seasons commonly. Thus, we can achieve a unified view of rainfall changes between the ocean, coastal area, and interior of Borneo by combining the datasets of OLR, 3B42, and the gauge network.

The gauge data clearly show that the DC strengthens during the MJO active phase and weakens during the break phase (no MJO disturbances), although phases of the DC are the same between coastal and interior regions. Rainfall increase is observed in all categories throughout the day in the active phase, but the diurnal rainfall pattern does not change between phases. The DC amplitude based on IR data decreased in the active phase over Borneo (Chen and Takahashi 1995) and the western

Pacific warm pool (Sui and Lau 1992). This is presumably because of reduced thermal contrast between land and ocean and broad areal coverage of clouds through the day during that period. However, the DCR based on gauge data clearly indicates enhanced rainfall in the active phase. TRMM PR data also show a weakened DC over land on the MC (Rauniyar and Walsh 2011), revealing an underestimated effect of the MJO on the DC, compatible with our result. The DC has large regional variability over land. Using TRMM 3B42 and IR datasets, Tian et al. (2006) showed that the DC is enhanced in the active phase between ocean and land across the MC, but the difference of MJO impact between land and ocean is small compared with our result. The maximum rainfall peak from IR data (Nitta and Sekine 1994; Chen and Takahashi 1995; Ohsawa et al. 2001; Chang et al. 2006) appears later by 2 or 3 h in comparison to the in situ data. The presence of anvil clouds is likely to cause this tendency in IR data (Nitta and Sekine 1994; Chen and Takahashi 1995; Ohsawa et al. 2001). In addition, the double peak of rainfall near the coast is not detected in these satellite data. The maximum rainfall peak of TRMM 3B42 is later than station data over southeast China (Yuan et al. 2012). Furthermore, this TRMM 3B42 peak is later than that of TRMM PR in the tropics (Kikuchi and Wang 2008). Consequently, this bias between rain gauge and TRMM data, which may be caused by anvil clouds, may exist in our study region. MJO disturbances strongly influence the coastal rainfall stations and nearby ocean; therefore, only the midnight-to-morning rainfall peak at the coastal stations was strengthened. Although the frequency of rainfall events increases in all categories during active phases, the intensity of each rainfall event changes only in the coastal land categories, during both phases. The afternoon rainfall maximum over the coastal region hardly changes between phases, but the intensity of this short-duration rainfall peak is stronger during the break phase. The DC differences between coastal and interior regions associated with the MJO are also evidenced in atmospheric circulation and thermodynamic instability. The low-level westerly wind anomaly, which is related to the active phase, transports more moisture to the interior region relative to the break phase. This increases atmospheric instability and the likelihood of rainfall events, based on local topography. In particular, the midnight-to-morning rainfall maxima at coastal stations strongly depend on large-scale convective activity of the MJO.

Thus, overall results of this study have shown that the MJO effect is relatively weak over the island interior, owing to the strong DC there during both active and break phases. During their passage over the MC, MJO convective cloud systems did not clearly change over land

compared with open seas (Hsu and Lee 2005; Wu and Hsu 2009). Houze et al. (1981) reported that in winter monsoon season, land breezes converge with low-level northeasterly monsoons to generate offshore convection. This develops into organized precipitation systems that drop heavy rainfall from midnight to morning over northwest Borneo. The northeasterly wind tends to shift to westerly through dynamic interaction of monsoon flow and orography over that area, presumably producing the convergence between low-level westerly and land breezes there. The low-level westerly anomaly in the active phase, therefore, intensifies this convergence and heavy rainfall around midnight over the coastal region. At that time, downslope wind occurrence may also be controlled by a mountain–valley wind system, as simulated for a case in southwest Borneo (called Kalimantan; Wu et al. 2008). Another possible mechanism may be the development of propagating storms along mountain slopes. This is triggered by the intrusion of cold air by gravity currents caused by interaction between the cold pool from the convection and ambient near-surface winds, as simulated by Satomura (2000). In addition to the propagating systems associated with the mountain range, gravity waves caused by a strong diurnal signal over coastal land would be important for propagation offshore (Yang and Slingo 2001; Mapes et al. 2003). The surface wind from land to coastal regions organized by these orographic processes may also interact with the land breeze around midnight. On the other hand, the enhanced afternoon rainfall peak associated with the increased rainfall frequency in the interior suggests an enhanced upslope wind, through a strengthened moist westerly wind during the active phase. The effect of the MJO on the DC over and around Borneo is thereby clearly different for ocean, coastal, and interior regions. It has been proposed that the DC rainfall peak propagates from the coastal to offshore region (Houze et al. 1981; Yang and Slingo 2001; Mapes et al. 2003; Yang and Smith 2006), which is likely intensified by the westerly wind anomaly during the active phase. To summarize the overall features of convection and rainfall over the South China Sea (SCS), coastal region, and interior of Borneo, we provide schematic drawings in Fig. 11.

In summary, the impact of MJO large-scale disturbances on the DC appears stronger in the midnight-to-morning rainfall maximum over coastal regions. More localized cloud/rain systems are dominant in the interior, during break and active phases. The DCR frequency increases over land because of increased water vapor transport from the nearby ocean and moist static instability. The DCR intensity is enhanced only in the coastal region during the active phase, modulated by large-scale cloud/rain systems of the MJO.
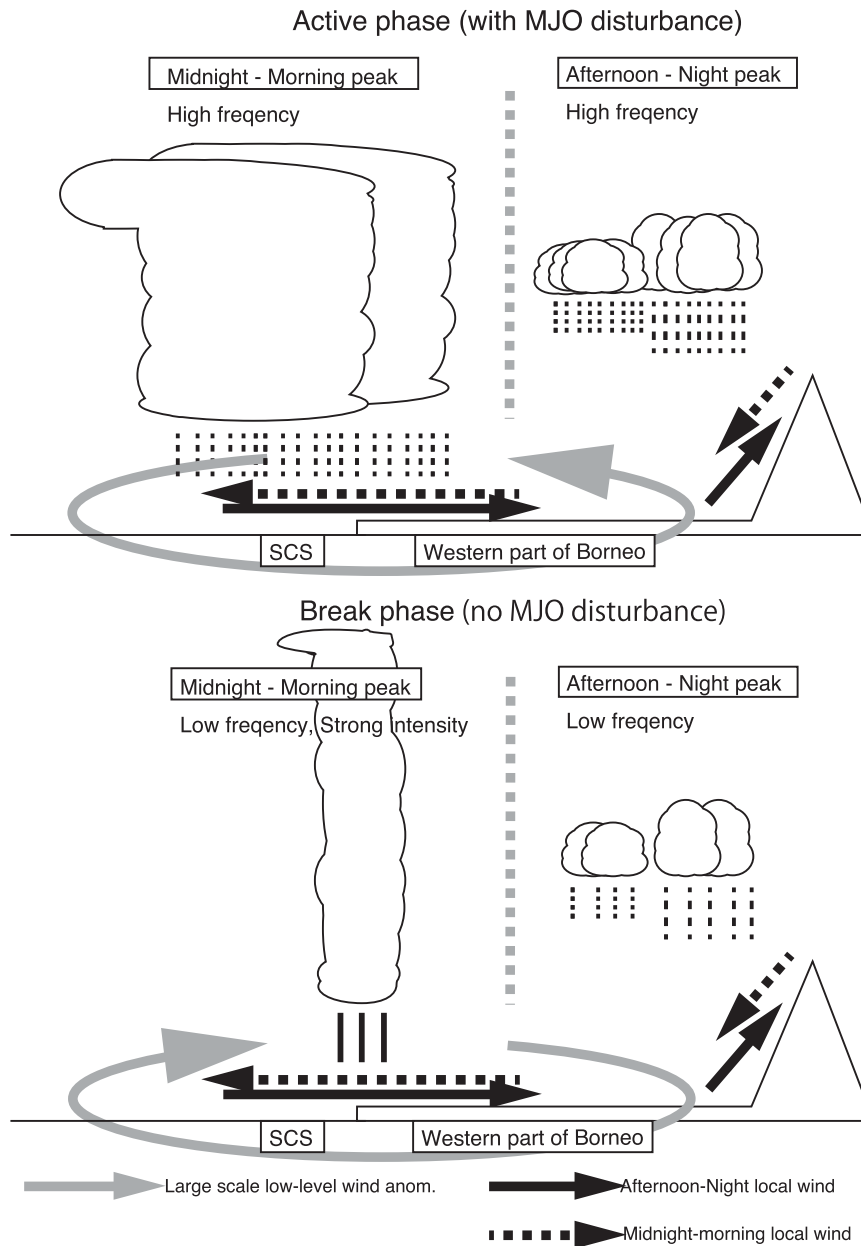
Active phase (with MJO disturbance)

Midnight - Morning peak

High freqency

Afternoon - Night peak

High freqency

SCS   Western part of Borneo

Break phase (no MJO disturbance)

Midnight - Morning peak

Low freqency, Strong intensity

Afternoon - Night peak

Low freqency

SCS   Western part of Borneo

Large scale low-level wind anom.   Afternoon-Night local wind

Midnight-morning local wind

FIG. 11. Diurnal schematics of rainfall and cloud systems over Sarawak: (top) active phase and (bottom) break phase. Gray arrows show large-scale, low-level circulation anomaly associated with the MJO. Black solid (dashed) arrows show local circulation winds that indicate land–sea breeze and mountain–valley circulations from afternoon to night (midnight to morning).

This variable influence of the MJO between coast and interior is very likely attributable to the differing effects of the land–sea breeze, mountainous orography, and land surface covered by tropical rain forest. How the enhanced DCR over Borneo associated with the MJO might change the MJO system itself could be another important issue of future study. A more intensive study,

including the meteorological radar network and numerical simulation by cloud-resolving climate models, would be necessary for such study.

REFERENCES

Chang, C.-P., P. A. Harr, and H. J. Chen, 2005a: Synoptic disturbances over the equatorial South China Sea and western Maritime Continent during boreal winter. *Mon. Wea. Rev.,* **133,** 489–503.

——, Z. Wang, J. McBride, and C. H. Liu, 2005b: Annual cycle of Southeast Asia–Maritime continent rainfall and the asymmetric monsoon transition. *J. Climate,* **18,** 287–301.

——, ——, and H. Hendon, 2006: The Asian winter monsoon. *The Asian Monsoon,* B. Wang, Ed., Praxis, 89–127.

Chen, T. C., and K. Takahashi, 1995: Diurnal variation of outgoing longwave radiation in the vicinity of the South China Sea: Effect of intraseasonal oscillation. *Mon. Wea. Rev.,* **123,** 566–577.

Gomyo, M., and K. Kuraji, 2006: Spatial distribution of seasonal variation in rainfall in the state of Sarawak, Malaysia (in Japanese with English abstract). *J. Japan. Soc. Hydrol. Water Resour.,* **19,** 128–138.

Hamada, J. I., M. D. Yamanaka, J. Matsumoto, S. Fukao, P. A. Winarso, and T. Sribimawati, 2002: Spatial and temporal variations of the rainy season over Indonesia and their link to ENSO. *J. Meteor. Soc. Japan,* **80,** 285–310.

——, ——, S. Mori, Y. I. Tauhid, and T. Sribimawati, 2008: Differences of rainfall characteristics between coastal and interior areas of central western Sumatera, Indonesia. *J. Meteor. Soc. Japan,* **86,** 593–611.

Houze, R. A., Jr., S. G. Geotis, F. D. Marks, and A. K. West, 1981: Winter monsoon convection in the vicinity of north Borneo. Part I: Structure and time variation of the clouds and precipitation. *Mon. Wea. Rev.,* **109,** 1595–1614.

Hsu, H.-H., and M.-Y. Lee, 2005: Topographic effects on the eastward propagation and initiation of the Madden–Julian oscillation. *J. Climate,* **18,** 795–809.

Huffman, G. J., and Coauthors, 2007: The TRMM multisatellite precipitation analysis (TMPA): Quasi-global, multiyear, combined-sensor precipitation estimates at fine scales. *J. Hydrometeor.,* **8,** 38–55.

Ichikawa, H., and T. Yasunari, 2006: Time–space characteristics of diurnal rainfall over Borneo and surrounding oceans as observed by TRMM-PR. *J. Climate,* **19,** 1238–1260.

Kikuchi, K., and B. Wang, 2008: Diurnal precipitation regimes in the global tropics. *J. Climate,* **21,** 2680–2696.

Kubota, T., S. Shige, K. Aonashi, and K. Okamoto, 2009: Development of nonuniform beamfilling correction method in rainfall retrievals for passive microwave radiometers over ocean using TRMM observations. *J. Meteor. Soc. Japan,* **87,** 153–164, doi:10.2151/jmsj.87a.153.

Kumagai, T., and Coauthors, 2005: Annual water balance and seasonality of evapotranspiration in a Bornean tropical rainforest. *Agric. For. Meteor.,* **128,** 81–92, doi:10.1016/j.agrformet.2004.08.006.

Kwon, E. H., B. J. Sohn, D. E. Chang, M. H. Ahn, and S. Yang, 2008: Use of numerical forecasts for improving TMI rain retrievals over the mountainous area in Korea. *J. Appl. Meteor. Climatol.,* **47,** 1995–2007.

Liebmann, B., and C. A. Smith, 1996: Description of a complete (interpolated) outgoing longwave radiation dataset. *Bull. Amer. Meteor.,* **77,** 1275–1277.

Lin, J. L., B. Mapes, M. Zhang, and M. Newman, 2004: Stratiform precipitation, vertical heating profiles, and the Madden–Julian oscillation. *J. Atmos. Sci.,* **61,** 296–309.

Madden, R. A., and P. R. Julian, 1971: Detection of a 40–50 day oscillation in zonal wind in tropical Pacific. *J. Atmos. Sci.,* **28,** 702–708.

——, and ——, 1972: Description of global-scale circulation cells in the tropics with a 40–50 day period. *J. Atmos. Sci.,* **29,** 1109–1123.

——, and ——, 1994: Observations of the 40–50-day tropical oscillation—A review. *Mon. Wea. Rev.,* **122,** 814–837.

Mapes, B. E., T. T. Warner, and M. Xu, 2003: Diurnal patterns of rainfall in northwestern South America. Part III: Diurnal gravity waves and nocturnal convection offshore. *Mon. Wea. Rev.,* **131,** 830–844.

Matsumoto, J., 1997: Seasonal transition of summer rainy season over Indochina and adjacent monsoon region. *Adv. Atmos. Sci.,* **14,** 231–245, doi:10.1007/s00376-997-0022-0.

Murakami, M., 1983: Analysis of the deep convective activity over the western Pacific and Southeast Asia. Part I: Diurnal variation. *J. Meteor. Soc. Japan,* **61,** 60–76.

Nair, S., G. Srinivasan, and R. Nemani, 2009: Evaluation of multisatellite TRMM derived rainfall estimates over a western state of India. *J. Meteor. Soc. Japan,* **87,** 927–939, doi:10.2151/jmsj.87.927.

Neale, R., and J. Slingo, 2003: The Maritime Continent and its role in the global climate: A GCM study. *J. Climate,* **16,** 834–848.

Nitta, T., and S. Sekine, 1994: Diurnal variation of convective activity over the tropical western Pacific. *J. Meteor. Soc. Japan,* **72,** 627–641.

Ohsawa, T., H. Ueda, T. Hayashi, A. Watanabe, and J. Matsumoto, 2001: Diurnal variations of connective activity and rainfall in tropical Asia. *J. Meteor. Soc. Japan,* **79,** 333–352.

Oki, T., and K. Musiake, 1994: Seasonal change of the diurnal cycle of precipitation over Japan and Malaysia. *J. Appl. Meteor.,* **33,** 1445–1463.

Onogi, K., and Coauthors, 2007: The JRA-25 reanalysis. *J. Meteor. Soc. Japan,* **85,** 369–432.

Ramage, C. S., 1968: Role of a tropical "maritime continent" in atmospheric circulation. *Mon. Wea. Rev.,* **96,** 365–370.

Rauniyar, S. P., and K. J. E. Walsh, 2011: Scale interaction of the diurnal cycle of rainfall over the Maritime Continent and Australia: Influence of the MJO. *J. Climate,* **24,** 325–348.

Satomura, T., 2000: Diurnal variation of precipitation over the Indo-China Peninsula: Two-dimensional numerical simulation. *J. Meteor. Soc. Japan,* **78,** 461–475.

Sui, C.-H., and K.-M. Lau, 1992: Multiscale phenomena in the tropical atmosphere over the western Pacific. *Mon. Wea. Rev.,* **120,** 407–430.

——, ——, Y. N. Takayabu, and D. A. Short, 1997: Diurnal variations in tropical oceanic cumulus convection during TOGA COARE. *J. Atmos. Sci.,* **54,** 639–655.

Tian, B. J., D. E. Waliser, and E. J. Fetzer, 2006: Modulation of the diurnal cycle of tropical deep convective clouds by the MJO. *Geophys. Res. Lett.,* **33,** L20704, doi:10.1029/2006GL027752.

Williams, M., and R. A. Houze, 1987: Satellite-observed characteristics of winter monsoon cloud clusters. *Mon. Wea. Rev.,* **115,** 505–519.

Wu, C.-H., and H.-H. Hsu, 2009: Topographic influence on the MJO in the Maritime Continent. *J. Climate,* **22,** 5433–5448.

Wu, P., M. D. Yamanaka, and J. Matsumoto, 2008: The formation of nocturnal rainfall offshore from convection over western Kalimantan (Borneo) Island. *J. Meteor. Soc. Japan,* **86,** 187–203.

Yang, G.-Y., and J. Slingo, 2001: The diurnal cycle in the tropics. *Mon. Wea. Rev.,* **129,** 784–801.

Yang, S., and E. A. Smith, 2006: Mechanisms for diurnal variability of global tropical rainfall observed from TRMM. *J. Climate,* **19,** 5190–5226.

Yuan, W., R. Yu, M. Zhang, W. Lin, H. Chen, and J. Li, 2012: Regimes of diurnal variation of summer rainfall over subtropical East Asia. *J. Climate,* **25,** 3307–3320.

Zhang, C., 2005: Madden–Julian oscillation. *Rev. Geophys.,* **43,** RG2003, doi:10.1029/2004RG000158.